Diffusion in Ionic Mixtures across Coupling Regimes

Jérôme Daligault*

Theoretical Division, Los Alamos National Laboratory, Los Alamos, New Mexico 87545, USA

(Received 22 March 2012; published 31 May 2012)

Molecular dynamics simulations are used to investigate the diffusion properties of one-component plasmas and binary ionic mixtures from the weakly to the strongly coupled regimes. A physically motivated model for the diffusivities is proposed that reproduces the simulation data and gives insight into the nature of ionic motions and interactions in plasmas across the coupling regimes. The model extends the widely used Chapman-Spitzer theory from the weakly to the moderately coupled regime. In the strongly coupled regime, diffusion is modeled in terms of thermally activated jumps between equilibrium positions separated by an energy barrier. The basic ideas discussed are applicable to the study of other transport coefficients.

DOI: 10.1103/PhysRevLett.108.225004 PACS numbers: 52.27.Gr, 52.25.Fi

High-fidelity computational modeling of many high-energy density laboratory experiments and astrophysical systems require accurate knowledge about the microscopic transport properties of plasma mixtures over a wide range of physical regimes. Of these properties, ionic transport coefficients such as diffusivities and viscosities play a critical role in various phenomena. For example, they are central to the modeling of inertial-confinement fusion imploding capsules since they affect the instability driven mixing of the heavy elements shell that encloses the lighter fuel [1] and influence the recently advanced plasma-physics effects [2]. In astrophysics, ionic transport is essential for understanding the composition of giant planets and for modeling the sedimentation of heavy elements in white dwarf stars and neutron stars' crusts that can strongly alter their light curves and nucleosynthesis [3]. All these physical systems, albeit involving very different chemical compositions, have in common a wide range of Coulomb couplings concurrently traversed from the weakly coupled regime studied in traditional plasma physics to the moderately and strongly coupled regimes where conventional estimates based upon, e.g., the Chapman-Spitzer (CS) theory [4–6], break down. In this Letter, we present an approach to the interpretation and modeling of the coefficients of ionic diffusion across the coupling regimes. We calculate the diffusion coefficients with molecular dynamics (MD) simulations on simple, but physically relevant plasma models over the entire range of coupling and for a large variety of compositions [7]. We validate the CS theory in the weakly coupled regime and extract the actual value of its *ad hoc* cutoff parameters. We show how the CS theory can be simply extended to the moderately coupled regime with no additional parameter. When ions are strongly coupled, the generalized CS theory breaks down but can be smoothly replaced by a model based upon the so-called "cage" effect.

Our MD simulations are based on a parallel implementation of the particle-particle particle-mesh algorithm that simultaneously treats long- and short-range encounters. The calculations are done with enough particles ($5000 \leq N \leq 200\,000$), over long enough time scales ($1638.4 \leq t\omega_p \leq 6553.6$) to ensure convergence with a statistical uncertainty of, at most, $\sim 5\%$ at the smallest couplings ($< 1\%$ elsewhere). Transport coefficients are calculated using Kubo formulas; e.g., the self-diffusion coefficient is $D = \frac{k_B T}{m} \int_0^\infty Z(t)$, where $Z(t)$ is the normalized velocity autocorrelation function (VAF) of the species considered [8]. The calculations are particularly demanding at small couplings due to a long collision mean-free path, which explains why *ab initio* validation of CS has been impractical before now. Previous MD data were collected at moderate and strong couplings and modeled with brute force, giving unphysical fits that are invalid outside the interpolation interval [3,9–11]. Besides CS-like theories [5,6], Rosenfeld, Nardi, and Zinamon [12] developed a practical model for strongly coupled binary ionic mixture (BIM) diffusivities in terms of those for effective hard spheres (with $\sim 30\%$ accuracy), but the model gives little insight into the underlying physics. A promising kinetic theoretic approximation to extend CS to higher coupling was described in Ref. [13].

We first consider the unmagnetized one-component plasma (OCP) model [14], a system of identical ions (mass m, charge $q = Ze$, density n, and plasmon frequency $\omega_p = \sqrt{4\pi q^2/m}$) at temperature T interacting through the Coulomb potential and immersed in a uniform neutralizing background. The OCP is characterized by the coupling parameter $\Gamma = q^2/ak_BT$, where $a = (4\pi n/3)^{-1/3}$ is the Wigner-Seitz radius. As Γ increases, the OCP changes from a nearly collisionless, gaseous regime for $\Gamma \ll 1$ through an increasingly correlated, liquid-like regime to the crystallization into a lattice at $\Gamma_m = q^2/ak_BT_m \approx 175$ [10]. Figure 1 shows our MD results for the self-diffusion coefficient D with $0.075 \leq \Gamma \leq \Gamma_m$ along with the model described below.

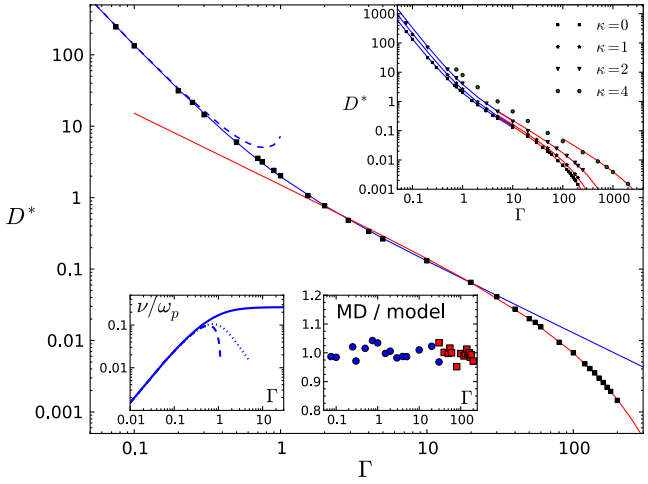

FIG. 1 (color online). Self-diffusion coefficient $D^* = D/a^2\omega_p$ of the OCP vs coupling Γ as obtained from MD (circles), along with the numerical fits to the data using (2) and (4) over $\Gamma < 2$. (blue line) and $50 \leq \Gamma$ (red line), respectively. The dashed line shows the $\Gamma \ll 1$ (CS) limit of (2). Top inset: same for the Yukawa OCP with $\kappa = 0, 1, 2, 4$ (from bottom to top). Bottom-left inset: generalized CS collision frequency (2) (for $\kappa = 0$) and its $\Gamma \ll 1$ limit (dashes). The dotted line shows the inadequacy of a commonly used ansatz to cure CS and based on the Rutherford scattering formula, $\ln\Lambda = 0.5\ln(1 + C^2\lambda_D^2/r_c^2)$ [6]. Bottom-right inset: ratio of MD and model data shown in main frame.

Elementary theories of diffusion assume binary collisions and lead to

$$D = \frac{1}{3} v_{\rm th} l_{\rm mfp} = \frac{k_B T}{m} \frac{1}{\nu}, \tag{1}$$

where $v_{\rm th}$ is the thermal velocity, $l_{\rm mfp} = v_{\rm th}/\nu$ the mean-free path, and ν the collision frequency. For weakly coupled plasmas, $\Gamma \ll 1$, the CS theory gives $\nu \equiv \nu_{\rm CS} = \nu_0 \ln\Lambda_{\rm CS}$, where $\nu_0 = \frac{4}{3}\sqrt{\pi/m}\frac{nq^4}{(k_B T)^{3/2}}$ and

$$\ln\Lambda_{\rm CS} = \ln\left(C\frac{\lambda_D}{r_L}\right) = \ln\left(\frac{C}{\sqrt{3}\Gamma^{3/2}}\right)$$

is the Coulomb logarithm. The latter arises because of the long-range nature of the Coulomb force and it is usually expressed in terms of the Debye length $\lambda_D = \sqrt{4\pi q^2 n/k_B T}$ (which represents the largest impact parameter beyond which interactions are screened out), and of the distance $r_L = q^2/k_B T$ (which characterizes the smallest impact parameter). C is a correction to these somewhat arbitrary cutoff parameters that is difficult to calculate analytically but, as we shall see, can be extracted from microscopic simulations ($C = 1$ is usually assumed). CS is clearly inapplicable when $\Gamma > (C/\sqrt{3})^{2/3}$, since it leads to negative diffusivities. We propose to extend the CS collision rate to higher coupling Γ as follows:

$$\nu = \alpha\nu_0 \ln\Lambda \quad \text{with} \quad \ln\Lambda = \ln\left(1 + C\frac{\lambda_D}{r_L}\right). \tag{2}$$

The factor α is a correction to the fact that $\nu_{\rm CS}$ corresponds to a single Sonine polynomial approximation in the Chapman-Enskog solution of the plasma kinetic equation [4]. The generalized Coulomb logarithm, $\ln\Lambda$, is always positive and reduces to $\ln\Lambda_{\rm CS}$ for $\Gamma \ll 1$. The blue line in Fig. 1 shows the result obtained with Eq. (2) when the parameters α, C are fitted to the MD data over the range $\Gamma \leq 2$, giving $\alpha = 0.647$ and $C = 2.159$. The model matches the data very well, and bridges the weakly and moderately coupled regimes up to $\Gamma \sim 30$, while the fit was done for $\Gamma \leq 2$. Our MD data validate the CS theory at small coupling $\Gamma \leq 0.2$ (dashed line in Fig. 1) and give access to the correction factors α and C. In the regime $4 \leq \Gamma \leq 30$, the collision frequency saturates at $\nu \approx 0.25\omega_p$ (see bottom inset of Fig. 1). Beyond $\Gamma \geq 30$, our extended CS model breaks down. As discussed in Refs. [10,15], the dynamics enter a distinctive, liquid-like regime where, pictorially, each particle finds itself trapped for some time in the cage formed by its immediate neighbors, and eventually escapes into a neighboring site when a thermal fluctuation helps it pass the energy barrier of the cage. By applying transition-state theory [16], Eyring obtained $D = \delta^2 k$, where δ is the distance between successive cages and

$$k = p\frac{k_B T}{h} e^{-\Delta F^*/k_B T} = p\frac{k_B T}{h} e^{\Delta S^*/k_B} e^{-\Delta U^*/k_B T} \tag{3}$$

is the frequency of jumps from cage to cage. Here, $p \leq 1$ is a transmission coefficient, and ΔS^* and ΔU^* are the entropy and energy of activation per ion (h is Planck's constant), respectively. In dimensionless units, the Eyring model reads [17]

$$D^* = \frac{D}{a^2\omega_p} = \frac{A}{\Gamma} e^{-B\Gamma} = \frac{A}{\Gamma} e^{-\gamma(T_m/T)} \tag{4}$$

in terms of two parameters A and B (or alternatively $\gamma = B\Gamma_m$), where we assume that ΔS^* and ΔU^* are independent of T over the small liquid regime $50 \leq \Gamma \leq \Gamma_m$. The red line in Fig. 1 shows the result obtained using Eq. (4) when A, B are fitted to the MD data over the range $50 \leq \Gamma \leq \Gamma_m$, yielding $A = 1.52$ and $B = 0.0082$. The model (4) matches the data remarkably well down to $\Gamma \sim 25$ where it merges with our generalized CS model. Interestingly, $\Gamma \sim 25$ roughly corresponds to the value at which the viscosity coefficient reaches a shallow minimum, separating the dense gas to the liquid-like regimes.

Similar agreement is found when the Coulomb potential is replaced by the Yukawa potential $e^{-\kappa r}/r$, where the inverse screening length, κ, mimics electronic screening [18]. This is illustrated in the inset of Fig. 1 for $\kappa a = 0$, 1, 2, and 4; the fitting parameters are collected in Table I and will be commented elsewhere.

TABLE I. Model parameters obtained by fitting the MD data shown in Fig. 1 (values of Γ_m at finite κ are taken from Ref. [18]). Note the relation $\Delta U^* \sim 1.2 - 1.4 k_B T_m$.

κa	Γ_m	α	C	A	$B = \Delta U^*/(q^2/a)$	γ
0	175.0	0.647	2.159	1.52	0.008 20	1.41
1	217.4	0.374	3.265	1.73	0.006 27	1.37
2	440.1	0.236	3.551	2.32	0.002 95	1.30
4	3837.			5.46	0.000 316	1.21

We now show that our approach extends to mixtures. We consider the binary ionic mixture model, consisting of two ionic species $j = 1, 2$ (charge $q_j = Z_j e$, mass m_j, number density n_j, concentration $x_j = n_j/n$, $n = n_1 + n_2$, and mass fraction X_j) at temperature T immersed in a uniform neutralizing background [19,20]. We find it convenient to characterize the BIM coupling strength by $\Gamma = \langle Z^{5/3}\rangle e^2/ak_BT$, where $\langle . \rangle$ is the number weighted average and $a = (3/4\pi n)^{1/3}$. A thorough study of BIMs is quite involved since BIMs depend on four parameters, e.g., m_1/m_2, Z_1/Z_2, x_1, and Γ, compared with only one for the OCP. In the weak to moderate coupling regime, we write the self-diffusion coefficient of each species as $D_j = \frac{k_BT}{m_j}\frac{1}{\nu_j}$ in terms of the collision frequency $\nu_j = \alpha_j \nu_0 \ln\Lambda_j$, and the Coulomb logarithm,

$$\ln\Lambda_j = \ln\left(1 + C_j \frac{\lambda_D}{r_c}\right) = \ln\left(1 + \frac{C_j'}{\Gamma^{3/2}}\right), \qquad (5)$$

with $\lambda_D = \sqrt{k_BT/4\pi n\langle q^2\rangle}$ and $r_c = \frac{q_1 q_2}{k_BT}$. For the reference frequency, ν_0, we choose that which was used in the CS inter-species collision frequency $\nu_{CS} = \nu_0 \ln\Lambda_{CS}$, where

$$\nu_0 = \frac{4}{3} n\sqrt{2\pi}\sqrt{\frac{\mu}{\langle m\rangle}}\frac{\langle m\rangle^2}{m_1 m_2}\frac{q_1^2 q_2^2}{(k_BT)^{3/2}}$$

and $\ln\Lambda_{CS} = \ln(C\lambda_D/r_c)$ (the Chapman calculation $C = 4$). For the strongly coupled regime, we again refer to the cage model and propose

$$D_j^* = \frac{D_j}{a^2\omega_p} = \frac{A_j}{\Gamma}\exp(-B_j\Gamma), \qquad (6)$$

where $\omega_p = \sqrt{4\pi\langle q\rangle^2/\langle m\rangle}$ is the plasmon frequency. Figure 2 shows a collection of results for D_1 and D_2 obtained for fully ionized H/D-, H/He-, He/C-, and H/C-like mixtures over a wide coupling range. The fitting parameters and their variation with the BIM parameters will be discussed elsewhere. The MD data show two distinctive regimes at small and large coupling that can be accurately reproduced by (5) and (6), respectively.

Our model for the self-diffusivities can be used to accurately estimate the mutual diffusion coeffcient $\mathcal{D}_{12} = \mathcal{J}D_{12}$ involved in Fick's law of diffusion [19], where $\mathcal{J}$

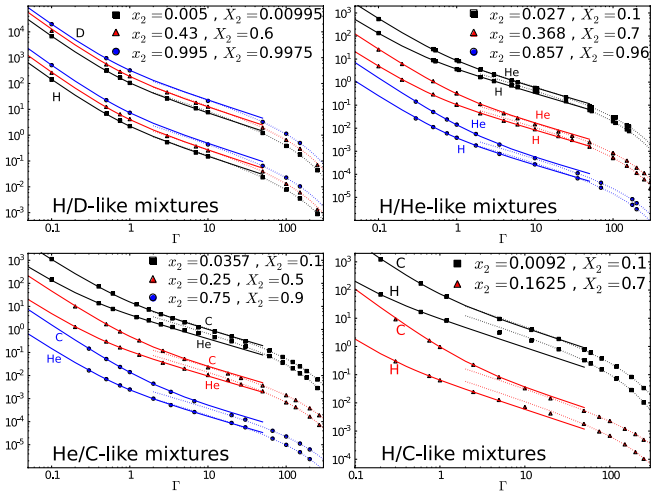

FIG. 2 (color online). Dimensionless self-diffusion coefficients $D_j/a^2\omega_p$ for various BIMs along with our model (see fitting parameters in Table II). For clarity, plots are shifted vertically [7].

is a thermodynamic factor ($\mathcal{J} = \langle Z^2\rangle/\langle Z\rangle^2$ at $\Gamma \ll 1$) [13] and $D_{12} = \frac{\langle m\rangle}{m_1 m_2}\frac{k_BT}{\nu_{12}}$ where ν_{12} is the friction [in CS, $\nu_{12} = \nu_0 \ln(4\lambda_D/r_c)$] [6]. Indeed, our MD data [7] confirm the previously established [12,13,19] empirical expression for D_{12} in a BIM in terms of the self-diffusion coefficients $D_{12} = x_2 D_1 + x_1 D_2$ of the same BIM (or, equivalently, $1/\nu_{12} = X_2/\nu_1 + X_1/\nu_2$). This mixing rule could potentially be extended to multicomponent mixtures.

The microscopic particle dynamics in BIMs are rich and varied, and its relation to transport properties on hydrodynamic scales is subtle. The study of isotopic mixtures, i.e., with $q_1 = q_2$ and $m_1 \le m_2$, provide a nice illustration of this. In isotopic mixtures, static particle distributions, like the pair-distribution functions, are all equal since they are mass independent. On the contrary, kinetic quantities like the momentum collisional exchanges are expected to depend on the mass ratio. We first consider the case in which species 2 is a trace element, i.e., $x_2 \ll 1$ and $m_2/m_1 = 2, 10, 100$ (see Table II). While the mass dependence of the diffusivities D_2 alluded to above is apparent, other noticeable features appear: with $x_2 = 0.005$, (i) $D_2(100) \approx D_2(10)$ for all Γ, i.e., the self-diffusivity of

TABLE II. Impurity self-diffusivities D_2 in isotopic BIMs in units of $a_1^2\omega_{p,1}$ independent of m_2 and x_2 to facilitate the comparisons.

x_2	$\frac{m_2}{m_1}$	$\Gamma = 0.5$	$\Gamma = 1$	$\Gamma = 50$	$\Gamma = 100$	$\Gamma = 150$
	2	5.54	1.87	0.0215	0.0067	0.00292
0.005	10	4.87	1.77	0.0210	0.0066	0.00288
	100	4.73	1.78	0.0206	0.0065	0.00284
	2	5.20	1.858	0.0190	0.005 90	0.002 95
0.111	10	3.98	1.459	0.0171	0.005 37	0.002 40
	100	2.61	0.933	0.0105	0.003 70	0.001 58

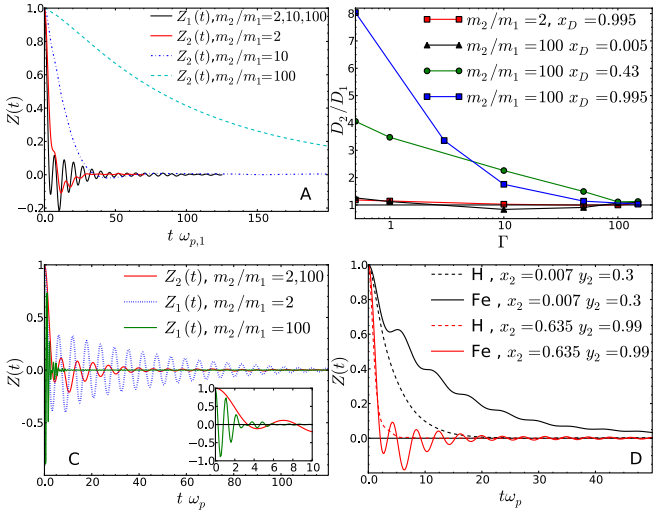

FIG. 3 (color online). (a) Comparison of VAFs in isotopic BIMs with a heavy trace element ($x_2 = 0.005$). (b) Variation with Γ of D_2/D_1 in isotopic BIMs. (c) Comparison of VAFs in isotopic mixtures with light impurities ($x_2 = 0.995$). (d) VAFs in fully ionized H/Fe-like mixtures.

a heavy impurity is nearly mass independent, while (ii) $D_2(2) \approx D_2(10) \approx D_2(100)$ at large Γ, i.e., the heavy impurity self-diffusivity is very weakly dependent on its mass in the liquid regime. The macroscopic dynamics, however, do not seemingly correlate with these findings; e.g., the VAFs are strongly mass dependent: in Fig. 3(a), $Z_2(t)$ oscillates and reaches negative values (caging) when $m_2/m_1 = 2$ but monotonically decays with no sign of strong-coupling effects when $m_2/m_1 = 100$. Fact (i) can be understood using the microscopic theory of Brownian motion [8]: for a heavy impurity $m_2 \gg m_1$ in a fluid of light particles,

$$\nu_2 = \frac{1}{3k_BTm_2}\int_0^\infty dt\langle \mathbf{f}(t)\cdot\mathbf{f}(0)\rangle_{\mathrm{eq}},$$

where $\mathbf{f}(t)$ is the force acting on a fixed impurity due to its interaction with the fluid light particles, $\langle . \rangle_{\mathrm{eq}}$ is the thermal average in the presence of the fixed impurity; the latter are independent of m_2 and so is $D_2 = k_BT/m_2\nu_2$ for all T, as found in our MD calculations. The data in Table II for $x_2 = 0.111$ show that the Brownian limit quickly breaks down since $D_2(10) \neq D_2(100)$. As x_2 increases, the light element self-diffusivity is also increasingly affected by the other species. However, Fig. 3(b) shows that the effect is much stronger at small coupling (e.g., when $x_2 = 0.43$ at $\Gamma = 0.5$, $D_2(100)/D_1 > 4$, while $D_2(2)/D_1 \approx 1.1$), while in the liquid regime (iii) $D_1 \approx D_2$ for all m_D, which is reminiscent of fact (ii) above. However, a look at the microscopic dynamics could suggest the contrary since, as illustrated in Fig. 3(c), the light species VAFs oscillate and vanish on very different time scales depending on m_2. A detailed Fourier analysis (not shown) [7,21] allows one to reconcile the microscopic and hydrodynamic behaviors. Shortly, in the liquid regime, a BIM supports collective, longitudinal, high-frequency (plasmon) excitations of wavelengths down to a few interparticle distances [22], and also sustains the propagation of shear waves with wavelengths of the order of the interpaticle separation. The former are responsible for the long-lived oscillatory behavior, but barely contribute to the zero-frequency component of the VAFs that gives the diffusivities (Kubo formula). On the hydrodynamic scale, however, self-diffusivities are determined almost entirely by the transverse modes. The same effect is at the origin of the Stokes-Einstein relation that relates diffusion and viscosity coefficients in all simple liquids and OCPs [10]. Of course, the diversity in the BIM's dynamics is even richer when both mass and charge ratios are varied. This is briefly illustrated in Fig. 3(d) that shows VAFs in asymmetric H/Fe-like mixture (relevant, e.g., to neutron stars). Here, because of its high electric charge ($Z_2/Z_1 = 26$), Fe ions can be strongly coupled among themselves (coupling is $\propto Z_2^2$), while H ions are weakly coupled to other H ions ($\propto Z_1^2$) and moderately coupled to Fe ions ($\propto Z_1Z_2$). Thus, H diffuses like in a weakly to moderately coupled plasma, while Fe diffusion is limited by strong coupling effects.

In summary, the Chapman-Spitzer result has been validated at small coupling and extended to moderate couplings by changing Λ_{CS} by $1 + \Lambda_{\mathrm{CS}}$ in the Coulomb logarithm. Remarkably, a similar extension was validated for a quite different relaxation mechanism, the temperature relaxation rates in electron-ion plasmas [23,24]. This strongly suggests that this extension of conventional plasma theory might be applicable to other plasma models (e.g., better screening model) and other transport properties (e.g., viscosities and conductivities). Recent progress in kinetic theory (e.g., [13,23,25]) may be useful to analytically predict the values of the parameters (such as α, C) without the need for demanding microscopic simulations.

This research is supported by the Department of Energy, under Contract No. W-7405-ENG-36.

*daligaul@lanl.gov

[1] S. Atzeni and J. Meyer-Ter-Vehn, *The Physics of Inertial Confinement Fusion* (Clarendon, Oxford, 2004).
[2] P. Amendt, O. L. Landen, H. F. Robey, C. K. Li, and R. D. Petrasso, Phys. Rev. Lett. **105**, 115005 (2010).
[3] C. J. Deloye and L. Bildsten, Astrophys. J. **580**, 1077 (2002); F. Peng, E. Brown, and J. W. Truran, Astrophys. J. **496**, 915 (1998), and references therein.
[4] S. Chapman and T. Cowling, *The Mathematical Theory of Non-Uniform Gases* (Cambridge University Press, Cambridge, England, 1970).
[5] L. Spitzer, *Physics of Fully Ionized Gases* (Wiley, New York, 1962).
[6] C. Paquette, C. Pelletier, G. Fontaine, and G. Michaud, Astrophys. J. Suppl. Ser. **61**, 177 (1986).

[7] Here we present the main conclusions of the study; a detailed report will appear elsewhere.
[8] U. Balucani and M. Zoppi, *Dynamics of the Liquid State* (Oxford University, New York, 1994).
[9] J. -P. Hansen, I. R. McDonald, and E. L. Pollock, Phys. Rev. A **11**, 1025 (1975).
[10] J. Daligault, Phys. Rev. Lett. **96**, 065003 (2006).
[11] H. Ohta and S. Hamaguchi, Phys. Plasmas **7**, 4506 (2000).
[12] Y. Rosenfeld, E. Nardi, and Z. Zinamon, Phys. Rev. Lett. **75**, 2490 (1995).
[13] D. B. Boercker and E. L. Pollock, Phys. Rev. A **36**, 1779 (1987).
[14] T. Ott and M. Bonitz, Phys. Rev. Lett. **107**, 135003 (2011).
[15] Z. Donko, G. J. Kalman, and K. I. Golden, Phys. Rev. Lett. **88**, 225001 (2002).
[16] S. Glasstone, K. J. Laidler, and H. Eyring, *Theory of Rate Processes* (McGraw-Hill, New York, 1941).
[17] To check the temperature dependence hypothesis, we have also considered the model $D^* = \frac{A}{\Gamma} e^{-B\Gamma} = \frac{A}{\Gamma^{**\alpha}} e^{-\gamma(T_m/T)}$ and obtained $\alpha = 1. \pm 0.006$.
[18] S. Hamaguchi, R. T. Farouki, and D. H. E. Dubin, Phys. Rev. E **56**, 4671 (1997).
[19] J.-P. Hansen, F. Joly, and I. R. McDonald, Physica (Amsterdam) **132A**, 472 (1985).
[20] S. Bastea, Phys. Rev. E **71**, 056405 (2005).
[21] T. Gaskell and S. Miller, J. Phys. C **11**, 3749 (1978); **11**, 4839 (1978).
[22] J. P. Mithen, J. Daligault, and G. Gregori, Phys. Rev. E **83**, 015401(R) (2011).
[23] J. Daligault and G. Dimonte, Phys. Rev. E **79**, 056403 (2009).
[24] G. Dimonte and J. Daligault, Phys. Rev. Lett. **101**, 135001 (2008).
[25] S. Baalrud, Phys. Plasmas **19**, 030701 (2012).